

A search for associated W and Higgs Boson production in $p\bar{p}$ collisions at $\sqrt{s} = 1.96$ TeV

V.M. Abazov³⁶, B. Abbott⁷⁵, M. Abolins⁶⁵, B.S. Acharya²⁹, M. Adams⁵¹, T. Adams⁴⁹, E. Aguilo⁶, M. Ahsan⁵⁹, G.D. Alexeev³⁶, G. Alkhazov⁴⁰, A. Alton^{64,a}, G. Alverson⁶³, G.A. Alves², M. Anastasoia³⁵, L.S. Ancu³⁵, T. Andeen⁵³, B. Andrieu¹⁷, M.S. Anzelc⁵³, M. Aoki⁵⁰, Y. Arnoud¹⁴, M. Arov⁶⁰, M. Arthaud¹⁸, A. Askew⁴⁹, B. Åsman⁴¹, A.C.S. Assis Jesus³, O. Atramentov⁴⁹, C. Avila⁸, F. Badaud¹³, L. Bagby⁵⁰, B. Baldin⁵⁰, D.V. Bandurin⁵⁹, P. Banerjee²⁹, S. Banerjee²⁹, E. Barberis⁶³, A.-F. Barfuss¹⁵, P. Bargassa⁸⁰, P. Baringer⁵⁸, J. Barreto², J.F. Bartlett⁵⁰, U. Bassler¹⁸, D. Bauer⁴³, S. Beale⁶, A. Bean⁵⁸, M. Begalli³, M. Begel⁷³, C. Belanger-Champagne⁴¹, L. Bellantoni⁵⁰, A. Bellavance⁵⁰, J.A. Benitez⁶⁵, S.B. Beri²⁷, G. Bernardi¹⁷, R. Bernhard²³, I. Bertram⁴², M. Besançon¹⁸, R. Beuselinck⁴³, V.A. Bezzubov³⁹, P.C. Bhat⁵⁰, V. Bhatnagar²⁷, C. Biscarat²⁰, G. Blazey⁵², F. Blekman⁴³, S. Blessing⁴⁹, K. Bloom⁶⁷, A. Boehlein⁵⁰, D. Boline⁶², T.A. Bolton⁵⁹, E.E. Boos³⁸, G. Borissov⁴², T. Bose⁷⁷, A. Brandt⁷⁸, R. Brock⁶⁵, G. Brooijmans⁷⁰, A. Bross⁵⁰, D. Brown⁸¹, X.B. Bu⁷, N.J. Buchanan⁴⁹, D. Buchholz⁵³, M. Buehler⁸¹, V. Buescher²², V. Bunichev³⁸, S. Burdin^{42,b}, T.H. Burnett⁸², C.P. Buszello⁴³, J.M. Butler⁶², P. Calfayan²⁵, S. Calvet¹⁶, J. Cammin⁷¹, E. Carrera⁴⁹, W. Carvalho³, B.C.K. Casey⁵⁰, H. Castilla-Valdez³³, S. Chakrabarti¹⁸, D. Chakraborty⁵², K.M. Chan⁵⁵, A. Chandra⁴⁸, E. Cheu⁴⁵, F. Chevallier¹⁴, D.K. Cho⁶², S. Choi³², B. Choudhary²⁸, L. Christofek⁷⁷, T. Christoudias⁴³, S. Cihangir⁵⁰, D. Claes⁶⁷, J. Clutter⁵⁸, M. Cooke⁵⁰, W.E. Cooper⁵⁰, M. Corcoran⁸⁰, F. Couderc¹⁸, M.-C. Cousinou¹⁵, S. Crépé-Renaudin¹⁴, V. Cuplov⁵⁹, D. Cutts⁷⁷, M. Ćwiok³⁰, H. da Motta², A. Das⁴⁵, G. Davies⁴³, K. De⁷⁸, S.J. de Jong³⁵, E. De La Cruz-Burelo³³, C. De Oliveira Martins³, K. DeVaughan⁶⁷, J.D. Degenhardt⁶⁴, F. Déliot¹⁸, M. Demarteau⁵⁰, R. Demina⁷¹, D. Denisov⁵⁰, S.P. Denisov³⁹, S. Desai⁵⁰, H.T. Diehl⁵⁰, M. Diesburg⁵⁰, A. Dominguez⁶⁷, H. Dong⁷², T. Dorland⁸², A. Dubey²⁸, L.V. Dudko³⁸, L. Duflot¹⁶, S.R. Dugad²⁹, D. Duggan⁴⁹, A. Duperrin¹⁵, J. Dyer⁶⁵, A. Dyshkant⁵², M. Eads⁶⁷, D. Edmunds⁶⁵, J. Ellison⁴⁸, V.D. Elvira⁵⁰, Y. Enari⁷⁷, S. Eno⁶¹, P. Ermolov^{38,‡}, H. Evans⁵⁴, A. Evdokimov⁷³, V.N. Evdokimov³⁹, A.V. Ferapontov⁵⁹, T. Ferbel⁷¹, F. Fiedler²⁴, F. Filthaut³⁵, W. Fisher⁵⁰, H.E. Fisk⁵⁰, M. Fortner⁵², H. Fox⁴², S. Fu⁵⁰, S. Fuess⁵⁰, T. Gadfort⁷⁰, C.F. Galea³⁵, C. Garcia⁷¹, A. Garcia-Bellido⁷¹, V. Gavrilov³⁷, P. Gay¹³, W. Geist¹⁹, W. Geng^{15,65}, C.E. Gerber⁵¹, Y. Gershtein⁴⁹, D. Gillberg⁶, G. Ginther⁷¹, N. Gollub⁴¹, B. Gómez⁸, A. Goussiou⁸², P.D. Grannis⁷², H. Greenlee⁵⁰, Z.D. Greenwood⁶⁰, E.M. Gregores⁴, G. Grenier²⁰, Ph. Gris¹³, J.-F. Grivaz¹⁶, A. Grohsjean²⁵, S. Grünendahl⁵⁰, M.W. Grünewald³⁰, F. Guo⁷², J. Guo⁷², G. Gutierrez⁵⁰, P. Gutierrez⁷⁵, A. Haas⁷⁰, N.J. Hadley⁶¹, P. Haefner²⁵, S. Hagopian⁴⁹, J. Haley⁶⁸, I. Hall⁶⁵, R.E. Hall⁴⁷, L. Han⁷, K. Harder⁴⁴, A. Harel⁷¹, J.M. Hauptman⁵⁷, J. Hays⁴³, T. Hebbeker²¹, D. Hedin⁵², J.G. Hegeman³⁴, A.P. Heinson⁴⁸, U. Heintz⁶², C. Hensel^{22,d}, K. Herner⁷², G. Hesketh⁶³, M.D. Hildreth⁵⁵, R. Hirosky⁸¹, J.D. Hobbs⁷², B. Hoeneisen¹², H. Hoeth²⁶, M. Hohlfeld²², S. Hossain⁷⁵, P. Houben³⁴, Y. Hu⁷², Z. Hubacek¹⁰, V. Hynek⁹, I. Iashvili⁶⁹, R. Illingworth⁵⁰, A.S. Ito⁵⁰, S. Jabeen⁶², M. Jaffré¹⁶, S. Jain⁷⁵, K. Jakobs²³, C. Jarvis⁶¹, R. Jesik⁴³, K. Johns⁴⁵, C. Johnson⁷⁰, M. Johnson⁵⁰, D. Johnston⁶⁷, A. Jonckheere⁵⁰, P. Jonsson⁴³, A. Juste⁵⁰, E. Kajfasz¹⁵, J.M. Kalk⁶⁰, D. Karmanov³⁸, P.A. Kasper⁵⁰, I. Katsanos⁷⁰, D. Kau⁴⁹, V. Kaushik⁷⁸, R. Kehoe⁷⁹, S. Kermiche¹⁵, N. Khalatyan⁵⁰, A. Khanov⁷⁶, A. Kharchilava⁶⁹, Y.M. Kharzeev³⁶, D. Khatidze⁷⁰, T.J. Kim³¹, M.H. Kirby⁵³, M. Kirsch²¹, B. Klima⁵⁰, J.M. Kohli²⁷, J.-P. Konrath²³, A.V. Kozelov³⁹, J. Kraus⁶⁵, T. Kuhl²⁴, A. Kumar⁶⁹, A. Kupco¹¹, T. Kurča²⁰, V.A. Kuzmin³⁸, J. Kvita⁹, F. Lacroix¹³, D. Lam⁵⁵, S. Lammers⁷⁰, G. Landsberg⁷⁷, P. Lebrun²⁰, W.M. Lee⁵⁰, A. Leflat³⁸, J. Lellouch¹⁷, J. Li^{78,‡}, L. Li⁴⁸, Q.Z. Li⁵⁰, S.M. Lietti⁵, J.K. Lim³¹, J.G.R. Lima⁵², D. Lincoln⁵⁰, J. Linnemann⁶⁵, V.V. Lipaev³⁹, R. Lipton⁵⁰, Y. Liu⁷, Z. Liu⁶, A. Lobodenko⁴⁰, M. Lokajicek¹¹, P. Love⁴², H.J. Lubatti⁸², R. Luna³, A.L. Lyon⁵⁰, A.K.A. Maciel², D. Mackin⁸⁰, R.J. Madaras⁴⁶, P. Mättig²⁶, C. Magass²¹, A. Magerkurth⁶⁴, P.K. Mal⁸², H.B. Malbouisson³, S. Malik⁶⁷, V.L. Malyshov³⁶, Y. Maravin⁵⁹, B. Martin¹⁴, R. McCarthy⁷², A. Melnitchouk⁶⁶, L. Mendoza⁸, P.G. Mercadante⁵, M. Merkin³⁸, K.W. Merritt⁵⁰, A. Meyer²¹, J. Meyer^{22,d}, J. Mitrevski⁷⁰, R.K. Mommsen⁴⁴, N.K. Mondal²⁹, R.W. Moore⁶, T. Moulik⁵⁸, G.S. Muanza²⁰, M. Mulhearn⁷⁰, O. Mundal²², L. Mundim³, E. Nagy¹⁵, M. Naimuddin⁵⁰, M. Narain⁷⁷, N.A. Naumann³⁵, H.A. Neal⁶⁴, J.P. Negret⁸, P. Neustroev⁴⁰, H. Nilsen²³, H. Nogima³, S.F. Novaes⁵, T. Nunnemann²⁵, V. O'Dell⁵⁰, D.C. O'Neil⁶, G. Obrant⁴⁰, C. Ochando¹⁶, D. Onoprienko⁵⁹, N. Oshima⁵⁰, N. Osman⁴³, J. Osta⁵⁵, R. Otec¹⁰, G.J. Otero y Garzón⁵⁰, M. Owen⁴⁴, P. Padley⁸⁰, M. Pangilinan⁷⁷, N. Parashar⁵⁶, S.-J. Park^{22,d}, S.K. Park³¹, J. Parsons⁷⁰, R. Partridge⁷⁷, N. Parua⁵⁴, A. Patwa⁷³, G. Pawloski⁸⁰, B. Penning²³, M. Perfilov³⁸, K. Peters⁴⁴, Y. Peters²⁶, P. Pétroff¹⁶, M. Petteni⁴³, R. Piegaia¹,

J. Piper⁶⁵, M.-A. Pleier²², P.L.M. Podesta-Lerma^{33,c}, V.M. Podstavkov⁵⁰, Y. Pogorelov⁵⁵, M.-E. Pol², P. Polozov³⁷, B.G. Pope⁶⁵, A.V. Popov³⁹, C. Potter⁶, W.L. Prado da Silva³, H.B. Prosper⁴⁹, S. Protopopescu⁷³, J. Qian⁶⁴, A. Quadt^{22,d}, B. Quinn⁶⁶, A. Rakitine⁴², M.S. Rangel², K. Ranjan²⁸, P.N. Ratoff⁴², P. Renkel⁷⁹, P. Rich⁴⁴, J. Rieger⁵⁴, M. Rijssenbeek⁷², I. Ripp-Baudot¹⁹, F. Rizatdinova⁷⁶, S. Robinson⁴³, R.F. Rodrigues³, M. Rominsky⁷⁵, C. Royon¹⁸, P. Rubinov⁵⁰, R. Ruchti⁵⁵, G. Safronov³⁷, G. Sajot¹⁴, A. Sánchez-Hernández³³, M.P. Sanders¹⁷, B. Sanghi⁵⁰, G. Savage⁵⁰, L. Sawyer⁶⁰, T. Scanlon⁴³, D. Schaire²⁵, R.D. Schamberger⁷², Y. Scheglov⁴⁰, H. Schellman⁵³, T. Schliephake²⁶, S. Schlobohm⁸², C. Schwanenberger⁴⁴, A. Schwartzman⁶⁸, R. Schwienhorst⁶⁵, J. Sekaric⁴⁹, H. Severini⁷⁵, E. Shabalina⁵¹, M. Shamim⁵⁹, V. Shary¹⁸, A.A. Shchukin³⁹, R.K. Shivpuri²⁸, V. Siccardi¹⁹, V. Simak¹⁰, V. Sirotenko⁵⁰, P. Skubic⁷⁵, P. Slattery⁷¹, D. Smirnov⁵⁵, G.R. Snow⁶⁷, J. Snow⁷⁴, S. Snyder⁷³, S. Söldner-Rembold⁴⁴, L. Sonnenschein¹⁷, A. Sopczak⁴², M. Sosebee⁷⁸, K. Soustruznik⁹, B. Spurlock⁷⁸, J. Stark¹⁴, J. Steele⁶⁰, V. Stolin³⁷, D.A. Stoyanova³⁹, J. Strandberg⁶⁴, S. Strandberg⁴¹, M.A. Strang⁶⁹, E. Strauss⁷², M. Strauss⁷⁵, R. Ströhmer²⁵, D. Strom⁵³, L. Stutte⁵⁰, S. Sumowidagdo⁴⁹, P. Svoisky⁵⁵, A. Sznaider³, P. Tamburello⁴⁵, A. Tanasijczuk¹, W. Taylor⁶, B. Tiller²⁵, F. Tissandier¹³, M. Titov¹⁸, V.V. Tokmenin³⁶, I. Torchiani²³, D. Tsybychev⁷², B. Tuchming¹⁸, C. Tully⁶⁸, P.M. Tuts⁷⁰, R. Unalan⁶⁵, L. Uvarov⁴⁰, S. Uvarov⁴⁰, S. Uzunyan⁵², B. Vachon⁶, P.J. van den Berg³⁴, R. Van Kooten⁵⁴, W.M. van Leeuwen³⁴, N. Varelas⁵¹, E.W. Varnes⁴⁵, I.A. Vasilyev³⁹, P. Verdier²⁰, L.S. Vertogradov³⁶, M. Verzocchi⁵⁰, D. Vilanova¹⁸, F. Villeneuve-Seguier⁴³, P. Vint⁴³, P. Vokac¹⁰, M. Voutilainen^{67,e}, R. Wagner⁶⁸, H.D. Wahl⁴⁹, M.H.L.S. Wang⁵⁰, J. Warchol⁵⁵, G. Watts⁸², M. Wayne⁵⁵, G. Weber²⁴, M. Weber^{50,f}, L. Welty-Rieger⁵⁴, A. Wenger^{23,g}, N. Wermes²², M. Wetstein⁶¹, A. White⁷⁸, D. Wicke²⁶, M. Williams⁴², G.W. Wilson⁵⁸, S.J. Wimpenny⁴⁸, M. Wobisch⁶⁰, D.R. Wood⁶³, T.R. Wyatt⁴⁴, Y. Xie⁷⁷, S. Yacoob⁵³, R. Yamada⁵⁰, W.-C. Yang⁴⁴, T. Yasuda⁵⁰, Y.A. Yatsunenko³⁶, H. Yin⁷, K. Yip⁷³, H.D. Yoo⁷⁷, S.W. Youn⁵³, J. Yu⁷⁸, C. Zeitnitz²⁶, S. Zelitch⁸¹, T. Zhao⁸², B. Zhou⁶⁴, J. Zhu⁷², M. Zielinski⁷¹, D. Ziemińska⁵⁴, A. Ziemiński^{54,†}, L. Zivkovic⁷⁰, V. Zutshi⁵², and E.G. Zverev³⁸

(*The DØ Collaboration*)

¹Universidad de Buenos Aires, Buenos Aires, Argentina

²LAFEX, Centro Brasileiro de Pesquisas Físicas, Rio de Janeiro, Brazil

³Universidade do Estado do Rio de Janeiro, Rio de Janeiro, Brazil

⁴Universidade Federal do ABC, Santo André, Brazil

⁵Instituto de Física Teórica, Universidade Estadual Paulista, São Paulo, Brazil

⁶University of Alberta, Edmonton, Alberta, Canada,

Simon Fraser University, Burnaby, British Columbia,

Canada, York University, Toronto, Ontario, Canada,

and McGill University, Montreal, Quebec, Canada

⁷University of Science and Technology of China, Hefei, People's Republic of China

⁸Universidad de los Andes, Bogotá, Colombia

⁹Center for Particle Physics, Charles University, Prague, Czech Republic

¹⁰Czech Technical University, Prague, Czech Republic

¹¹Center for Particle Physics, Institute of Physics,

Academy of Sciences of the Czech Republic, Prague, Czech Republic

¹²Universidad San Francisco de Quito, Quito, Ecuador

¹³LPC, Université Blaise Pascal, CNRS/IN2P3, Clermont, France

¹⁴LPSC, Université Joseph Fourier Grenoble 1, CNRS/IN2P3,

Institut National Polytechnique de Grenoble, Grenoble, France

¹⁵CPPM, Aix-Marseille Université, CNRS/IN2P3, Marseille, France

¹⁶LAL, Université Paris-Sud, IN2P3/CNRS, Orsay, France

¹⁷LPNHE, IN2P3/CNRS, Universités Paris VI and VII, Paris, France

¹⁸CEA, Irfu, SPP, Saclay, France

¹⁹IPHC, Université Louis Pasteur, CNRS/IN2P3, Strasbourg, France

²⁰IPNL, Université Lyon 1, CNRS/IN2P3, Villeurbanne, France and Université de Lyon, Lyon, France

²¹III. Physikalisches Institut A, RWTH Aachen University, Aachen, Germany

²²Physikalisches Institut, Universität Bonn, Bonn, Germany

²³Physikalisches Institut, Universität Freiburg, Freiburg, Germany

²⁴Institut für Physik, Universität Mainz, Mainz, Germany

²⁵Ludwig-Maximilians-Universität München, München, Germany

²⁶Fachbereich Physik, University of Wuppertal, Wuppertal, Germany

²⁷Panjab University, Chandigarh, India

²⁸Delhi University, Delhi, India

²⁹Tata Institute of Fundamental Research, Mumbai, India

³⁰University College Dublin, Dublin, Ireland
³¹Korea Detector Laboratory, Korea University, Seoul, Korea
³²SungKyunKwan University, Suwon, Korea
³³CINVESTAV, Mexico City, Mexico
³⁴FOM-Institute NIKHEF and University of Amsterdam/NIKHEF, Amsterdam, The Netherlands
³⁵Radboud University Nijmegen/NIKHEF, Nijmegen, The Netherlands
³⁶Joint Institute for Nuclear Research, Dubna, Russia
³⁷Institute for Theoretical and Experimental Physics, Moscow, Russia
³⁸Moscow State University, Moscow, Russia
³⁹Institute for High Energy Physics, Protvino, Russia
⁴⁰Petersburg Nuclear Physics Institute, St. Petersburg, Russia
⁴¹Lund University, Lund, Sweden, Royal Institute of Technology and Stockholm University, Stockholm, Sweden, and Uppsala University, Uppsala, Sweden
⁴²Lancaster University, Lancaster, United Kingdom
⁴³Imperial College, London, United Kingdom
⁴⁴University of Manchester, Manchester, United Kingdom
⁴⁵University of Arizona, Tucson, Arizona 85721, USA
⁴⁶Lawrence Berkeley National Laboratory and University of California, Berkeley, California 94720, USA
⁴⁷California State University, Fresno, California 93740, USA
⁴⁸University of California, Riverside, California 92521, USA
⁴⁹Florida State University, Tallahassee, Florida 32306, USA
⁵⁰Fermi National Accelerator Laboratory, Batavia, Illinois 60510, USA
⁵¹University of Illinois at Chicago, Chicago, Illinois 60607, USA
⁵²Northern Illinois University, DeKalb, Illinois 60115, USA
⁵³Northwestern University, Evanston, Illinois 60208, USA
⁵⁴Indiana University, Bloomington, Indiana 47405, USA
⁵⁵University of Notre Dame, Notre Dame, Indiana 46556, USA
⁵⁶Purdue University Calumet, Hammond, Indiana 46323, USA
⁵⁷Iowa State University, Ames, Iowa 50011, USA
⁵⁸University of Kansas, Lawrence, Kansas 66045, USA
⁵⁹Kansas State University, Manhattan, Kansas 66506, USA
⁶⁰Louisiana Tech University, Ruston, Louisiana 71272, USA
⁶¹University of Maryland, College Park, Maryland 20742, USA
⁶²Boston University, Boston, Massachusetts 02215, USA
⁶³Northeastern University, Boston, Massachusetts 02115, USA
⁶⁴University of Michigan, Ann Arbor, Michigan 48109, USA
⁶⁵Michigan State University, East Lansing, Michigan 48824, USA
⁶⁶University of Mississippi, University, Mississippi 38677, USA
⁶⁷University of Nebraska, Lincoln, Nebraska 68588, USA
⁶⁸Princeton University, Princeton, New Jersey 08544, USA
⁶⁹State University of New York, Buffalo, New York 14260, USA
⁷⁰Columbia University, New York, New York 10027, USA
⁷¹University of Rochester, Rochester, New York 14627, USA
⁷²State University of New York, Stony Brook, New York 11794, USA
⁷³Brookhaven National Laboratory, Upton, New York 11973, USA
⁷⁴Langston University, Langston, Oklahoma 73050, USA
⁷⁵University of Oklahoma, Norman, Oklahoma 73019, USA
⁷⁶Oklahoma State University, Stillwater, Oklahoma 74078, USA
⁷⁷Brown University, Providence, Rhode Island 02912, USA
⁷⁸University of Texas, Arlington, Texas 76019, USA
⁷⁹Southern Methodist University, Dallas, Texas 75275, USA
⁸⁰Rice University, Houston, Texas 77005, USA
⁸¹University of Virginia, Charlottesville, Virginia 22901, USA and
⁸²University of Washington, Seattle, Washington 98195, USA

(Dated: August 14th 2008)

We present results of a search for $WH \rightarrow \ell\nu b\bar{b}$ production in $p\bar{p}$ collisions based on the analysis of 1.05 fb^{-1} of data collected by the D0 experiment at the Fermilab Tevatron, using a neural network for separating the signal from backgrounds. No signal-like excess is observed, and we set 95% C.L. upper limits on the WH production cross section multiplied by the branching ratio for $H \rightarrow b\bar{b}$ for Higgs boson masses between 100 and 150 GeV. For a mass of 115 GeV, we obtain an observed (expected) limit of 1.5 (1.4) pb, a factor of 11.4 (10.7) times larger than standard model prediction.

The Higgs boson is the last unobserved particle of the standard model (SM). As a remnant of spontaneous electroweak symmetry breaking, it is fundamentally different from the other elementary particles, and its observation would support the hypothesis that the Higgs mechanism generates the masses of the weak gauge bosons and the charged fermions. The Higgs boson mass (m_H) is not theoretically predicted, but the combination of results from direct searches at the CERN LEP collider [1] with the indirect constraints from precision electroweak measurements results in a preferred range of $114.4 < m_H < 190$ GeV at 95% C.L [2]. Such mass range can be probed at the Fermilab Tevatron collider. In this Letter, we concentrate on the most sensitive production channel at the Tevatron for Higgs bosons of mass below 125 GeV, i.e. the associated production of a Higgs boson with a W boson. Several searches for WH production have been published at a center-of-mass energy of $\sqrt{s} = 1.96$ TeV. Two [3, 4] used subsamples (0.17 fb^{-1} and 0.44 fb^{-1}) of the data reported in this Letter, while two others, from the CDF collaboration, are based on 0.32 fb^{-1} and 0.95 fb^{-1} of integrated luminosity [5, 6].

This analysis uses 1.05 fb^{-1} of D0 [7, 8] data, collected between April 2002 and February 2006. As in our previous WH analyses [3, 4], we require one high transverse momentum (p_T) lepton (e or μ) and missing transverse energy \cancel{E}_T to account for the neutrino from the W boson decay, and two jets from the decay of the Higgs boson, with at least one of them being identified as originating from a bottom (b) quark jet. We extend this data selection by including also events with three jets and events with “forward” electrons detected at pseudorapidities [9] $|\eta| > 1.5$. We also now accept the small contribution originating from misreconstructed ZH , in which only one lepton from the Z is identified. In addition we use a more inclusive trigger selection in the muon channel, increasing the detection efficiency from approximately 70% to 100% [10], we improve the b -jet identification using a neural network algorithm [11], and we enhance the signal to background discrimination using a neural network for the $W + 2$ jet events. Overall, the improvements in analysis techniques have led to an increase of about 40% in the sensitivity (for an equivalent luminosity) to a Higgs boson with mass 115 GeV, with respect to our previous analysis [4].

For the e channel, the $W +$ jets candidate events are collected, with $\approx 90\%$ efficiency, by triggers that require at least one electromagnetic (EM) object in the calorimeter. In the μ channel, $\approx 90\%$ of the candidates are collected by triggers requiring a single muon or a muon plus a jet, while the remaining 10% of events are collected by other triggers, for a total trigger efficiency of $\approx 100\%$, as estimated in data [10].

The event selection requires one lepton candidate with $p_T > 15 \text{ GeV}$, $\cancel{E}_T > 20 \text{ GeV}$ ($\cancel{E}_T > 25 \text{ GeV}$ for events with a forward electron), and exactly two jets with $p_T > 25$

and 20 GeV, and $|\eta| < 2.5$, or exactly three jets with $p_T > 25, 20$ and 20 GeV, and $|\eta| < 2.5$. We also require the scalar sum of the p_T of the jets to be $> 60 \text{ GeV}$, the W transverse mass M_W^T reconstructed from the \cancel{E}_T and the lepton p_T to be greater than $40 \text{ GeV} - 0.5 \times \cancel{E}_T$ to reject multijet background, and the primary interaction vertex to take place within the longitudinal acceptance of the vertex detector. Jets are reconstructed using a midpoint cone algorithm [12] with a radius of 0.5. The \cancel{E}_T is calculated from energies in calorimeter cells and corrected for the p_T of identified muons. All energy corrections applied to electrons or jets are also propagated to the \cancel{E}_T .

A central (forward) electron is required to have $|\eta| < 1.1$ ($1.5 < |\eta| < 2.5$). To reject fake electrons originating mostly from instrumental effects (track-photon overlap), the electron candidates must satisfy two sets of identification (“loose” and “tight”) criteria [4]. The efficiencies of these requirements are determined from a pure sample of $Z \rightarrow e^+e^-$ events. The differential multijet background for every relevant distribution is then estimated from the loose and tight lepton samples [4, 13]. The same statistical method is used for muons, but with different loose/tight definitions. Muons are reconstructed using information from the outer muon detector and the central tracker, and must have $|\eta| < 2.0$. To reject muons originating from semi-leptonic decays of heavy-flavor hadrons, we exploit the fact that they have lower p_T than those originating from W decay, and are generally not isolated because of accompanying jet fragments. The loose isolation criterion is thus defined by specifying a spatial separation between a muon and the closest jet in the η - φ plane of $\Delta R = \sqrt{(\Delta\eta)^2 + (\Delta\varphi)^2} > 0.5$, where φ is the azimuthal angle. Tighter isolation is defined by requiring little tracking and calorimetric activity around the muon track.

The dominant backgrounds to WH production are from $W +$ heavy flavor jets production, top quark pair production ($t\bar{t}$), and single top quark production. Signal (WH and ZH) and diboson processes (WW , WZ , ZZ) are simulated using the PYTHIA [14] event generator, and CTEQ6L [15] leading-order parton distribution functions. “ $W +$ jets” events refer to W bosons produced in association with light-flavor jets (originating from u , d , s quarks or gluons) or charm jets (originating from c quarks), and constitute the dominant background before b -jet identification. $Wc\bar{c}$ and $Wb\bar{b}$ are simulated individually and associated as “ $Wb\bar{b}$ ” for purposes of accounting. These W boson processes are generated with ALPGEN [16] interfaced to PYTHIA for showering and fragmentation, since ALPGEN provides a more complete simulation of processes with high jet multiplicities than PYTHIA. The $t\bar{t}$ and $Z +$ jets, events are also generated using ALPGEN/PYTHIA. The production of single top quarks is simulated with COMPHEP [17].

The simulated backgrounds are normalized to their re-

spective NLO theoretical cross sections, with the exception of the $W +$ jets and $W +$ heavy-flavor samples, which are normalized to data after subtraction of all the other backgrounds, before b -jet identification. All generated events are processed through the D0 detector simulation based on GEANT [18]. Data collected with a random bunch crossing trigger are overlaid on the simulated events to model the occupancy of the detector which is dependent on the instantaneous luminosity. The resulting events are then passed through the reconstruction software. Finally, corrections are applied to account for the trigger efficiency and for residual discrepancies between the data and the simulation.

We use a neural network b -tagging (NN_b) algorithm [11] to identify heavy-flavor jets. Its requirements are optimized for the best sensitivity to the Higgs boson signal. For each jet multiplicity, we form two statistically independent samples, one (2 b -tag) with two b -tagged jets using a loose NN_b criterion resulting in a b -jet efficiency of 59% and a light-jet tagging (mistag) probability of 1.7%, and a second (1 b -tag) with exactly one b -tagged jet using a tighter NN_b criterion (48% efficiency and 0.5% mistag probability). All efficiencies are determined for jets satisfying minimum requirements in terms of track quality and multiplicity (“taggable jets”), which constitute $\approx 80\%$ of all jets. In the simulations, the b -tagged jets are weighted to reproduce the tagging rate measured in data samples.

Using these selection criteria, we observe 885 (385) in the 1 b -tag $W + 2$ jet ($W + 3$ jet) samples and 136 (122) events in the corresponding 2 b -tag sample. Distributions of the dijet invariant mass, using the two jets of highest p_T , in $W + 2$ jet and $W + 3$ jet events are shown for the 1 b -tag and 2 b -tag samples in Fig. 1(a–d). The data are well described by the sum of the simulated SM processes and multijet background. The expected contributions from a Higgs boson with $m_H = 115$ GeV are also shown. The expected event yields for the backgrounds and a Higgs boson with $m_H = 115$ GeV are compared to the observed number of events in Table I.

Although the dijet invariant mass is a powerful variable for separating a Higgs boson signal from background [4], the sensitivity of the analysis is enhanced through the use of multivariate techniques: in $W + 2$ jet events, a neural network is trained on simulated signal and $Wb\bar{b}$ events, using seven kinematic variables: p_T of the highest and second-highest p_T jet, $\Delta R(\text{jet}_1, \text{jet}_2)$, $\Delta\varphi(\text{jet}_1, \text{jet}_2)$, $p_T(\text{dijet system})$, dijet invariant mass, and $p_T(W$ boson candidate). The training is performed for every simulated Higgs signal (different test masses), and separately for e , μ , 1 b -tag and 2 b -tag events. The resulting neural networks are then applied to $W + 2$ jet data and to the background and simulated signal samples. In the final limit-setting procedure, the distributions of the neural network discriminant corresponding to a specific Higgs boson test mass are used for analyzing the $W + 2$ jet

events. The improvement in sensitivity over just using the dijet invariant mass is about 15% at $m_H = 115$ GeV. The resulting neural network discriminants are shown in Fig. 1(e,f). For the $W + 3$ jet samples, whose dominant background is $t\bar{t}$, the limits are determined directly from the dijet mass distributions.

Systematic uncertainties on efficiencies and from the propagation of other systematics (e.g. energy calibration and detector response) are: (3–5)% for trigger efficiency; (4–5)% for lepton identification efficiency; 6% for jet identification efficiency and jet resolution; 5% from the modeling of the jet multiplicity spectrum; 3% due to the uncertainty in the jet energy calibration; 2–10% due to the uncertainty in modeling $W +$ jets, determined by comparing data and expectation before b -tagging and before reweighting the $W +$ jet samples to match the data

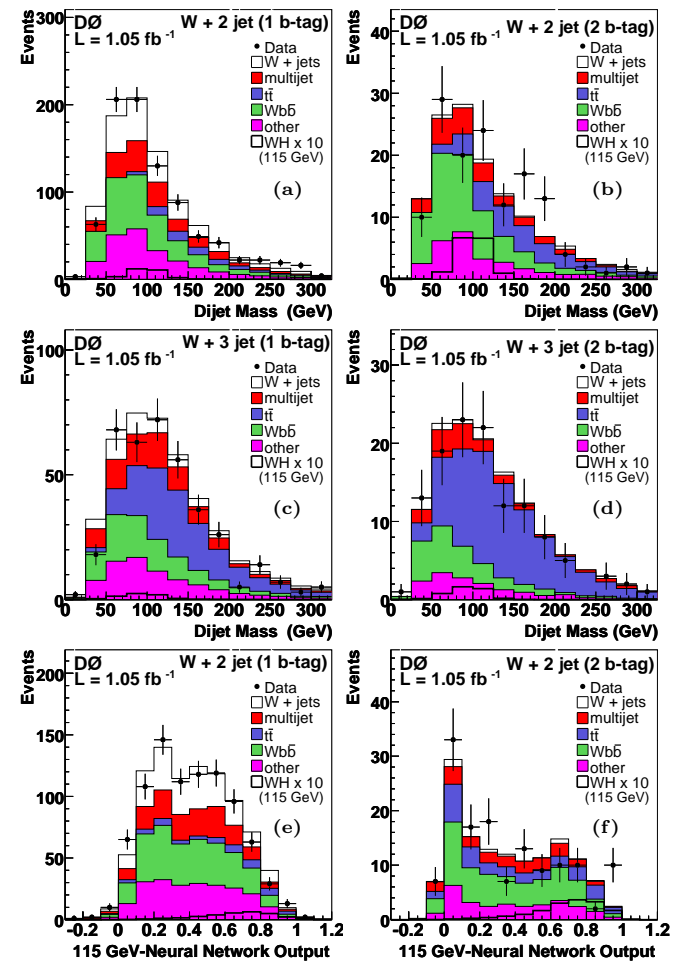


FIG. 1: Dijet mass distributions for the $W + 2$ jet, $W + 3$ jet 1 b -tag events (a,c) and 2 b -tag (b,d) events. The data are compared to the background prediction. The distributions in the neural network discriminant for $W + 2$ jet 1 b -tag and 2 b -tag events are shown in (e,f), respectively. The expectation from $WH(x10)$ production for $m_H = 115$ GeV is overlaid (color online).

TABLE I: Summary of event yields for the ℓ (e and μ) + b -tagged jets + \cancel{E}_T final state. Events in data are compared with the expected number of 1 b -tag and 2 b -tag events in the $W+2$ and $W+3$ jet samples, in simulated samples of diboson (labelled “ WZ ” in the table), $W/Z+b\bar{b}$ or $c\bar{c}$ (“ $Wb\bar{b}$ ”), $W/Z+$ light quark jets (“ $W+jets$ ”), top quark (“ $t\bar{t}$ ” and “single t ”) production, and multijet background (“m-jet”) determined from data (see text). The WH expectation is given for $m_H = 115$ GeV, and not included in the “Total” SM expectation.

	$W + 2$ jet 1 b -tag	$W + 2$ jet 2 b -tag	$W + 3$ jet 1 b -tag	$W + 3$ jet 2 b -tag
WH	2.8 ± 0.3	1.5 ± 0.2	0.7 ± 0.1	0.4 ± 0.1
WZ	34.5 ± 3.7	5.3 ± 0.6	9.1 ± 1.0	1.7 ± 0.2
$Wb\bar{b}$	268 ± 67	54 ± 14	87 ± 22	22.7 ± 5.7
$W+jets$	347 ± 87	14.0 ± 4.4	96 ± 24	8.5 ± 2.7
$t\bar{t}$	95 ± 17	37.4 ± 7.0	156 ± 29	81 ± 15
single t	49.4 ± 9.0	12.4 ± 2.3	15.7 ± 2.9	6.7 ± 1.2
m-jet	104 ± 29	8.9 ± 2.1	54 ± 15	8.7 ± 2.1
Total	896 ± 177	132 ± 27	418 ± 76	129 ± 24
Data	885	136	385	122

(the effect of this uncertainty on the shape of the neural network discriminant is also taken into account); 3% for jet taggability; and 2% uncertainty for b -tagging efficiency. For light quark jets, the uncertainty on the mistag rate is 15%. The multijet background, determined from data, has an uncertainty of 18–38%. The systematic uncertainty on the theoretical cross section for the simulated backgrounds is 6–20%, depending on the process. The uncertainty on the luminosity is 6% [19].

We use the CLs method [20, 21] to assess the compatibility of data with the presence of a Higgs signal. In the absence of any significant enhancement, we obtain upper limits on WH production, using the neural network output (dijet invariant mass of the $b\bar{b}$ system) for the $W + 2$ jet ($W + 3$ jet) sample as the final discriminating variable. The 1 b -tag and 2 b -tag, and the e and μ channels, are treated separately, giving a total of eight analyses, which are then combined [4]. We incorporate systematic uncertainties on signal and background expectations using Gaussian sampling and include correlations among the uncertainties across the analysis channels. We reduce the impact of systematic uncertainties using the profile likelihood technique [21].

The combined upper limits obtained at the 95% C.L. on $\sigma(p\bar{p} \rightarrow WH) \times B(H \rightarrow b\bar{b})$ are displayed in Fig. 2 and given in Table II, together with the ratios of these limits to the predicted SM cross section. For this analysis, all deviations between observed and expected limits are less than 1.5 standard deviations. At $m_H = 115$ GeV, the observed (expected) limits are 1.5 (1.4) pb, or a factor of 11.4 (10.7) times higher than the SM prediction. Our new limits are displayed in Fig. 2 and compared to the expected limit from our previous analysis [4]. The im-

TABLE II: Observed and expected 95% C.L. upper limits on the cross section times branching fraction ($\sigma \times B$) in pb, where $B = B(H \rightarrow b\bar{b})$, for different Higgs boson mass values; the corresponding ratios to the predicted SM cross section are also given.

m_H [GeV]	100	105	110	115	120	125	130	135	140	145	150
exp. $\sigma \times B$	1.66	1.53	1.44	1.36	1.25	1.19	1.13	1.16	1.09	1.01	1.01
obs. $\sigma \times B$	2.07	2.08	1.80	1.46	1.54	1.21	1.15	1.12	1.46	1.10	0.95
exp. ratio	7.3	8.0	9.2	10.7	12.3	15.1	19.1	27.3	37.4	53.5	90.2
obs. ratio	9.1	11.0	11.5	11.4	15.1	15.3	19.5	26.4	50.1	58.2	83.9

provement in sensitivity is significant, and our expected limits scale approximately inversely with luminosity compared to our previous result. These limits are the most stringent to date in this process at a hadron collider.

In summary, we have presented 95% C.L. upper limits on the product of $WH \rightarrow \ell\nu b\bar{b}$ production cross section and branching fraction for $H \rightarrow b\bar{b}$. These range between 2.1 and 1.0 pb for $100 < m_H < 150$ GeV, while the corresponding SM predictions range from 0.23 to 0.01 pb. The sensitivity should increase significantly in the near future with the continuing accumulation of luminosity from the Tevatron and improvement in analysis techniques. A significant sensitivity gain has already been achieved by combining these data, with other Higgs boson searches done by the CDF and D0 collaborations [22].

We thank the staffs at Fermilab and collaborating institutions, and acknowledge support from the DOE and NSF (USA); CEA and CNRS/IN2P3 (France);

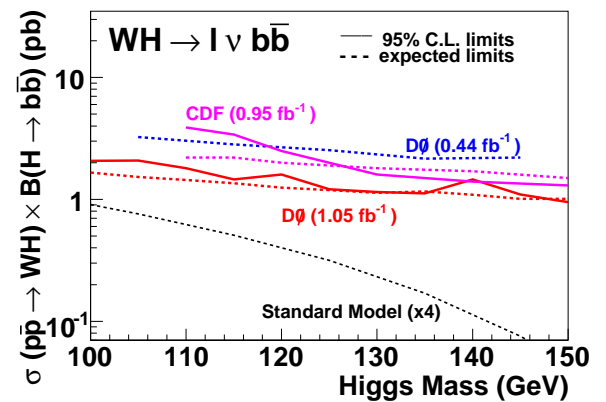


FIG. 2: 95% C.L. cross section upper limit (and corresponding expected limit) on $\sigma(p\bar{p} \rightarrow WH) \times B(H \rightarrow b\bar{b})$ vs. Higgs boson mass, compared to the SM expectation and to the expected limit from our previous analysis [4]. Recent CDF results [6] are also shown. Solid (dashed) lines represent observed (expected) limits. The contribution of ZH reconstructed in the same final state is taken into account in the WH signal when deriving the limits, assuming the SM ratio of ZH/WH cross sections.

FASI, Rosatom and RFBR (Russia); CNPq, FAPERJ, FAPESP and FUNDUNESP (Brazil); DAE and DST (India); Colciencias (Colombia); CONACyT (Mexico); KRF and KOSEF (Korea); CONICET and UBACyT (Argentina); FOM (The Netherlands); STFC (United Kingdom); MSMT and GACR (Czech Republic); CRC Program, CFI, NSERC and WestGrid Project (Canada); BMBF and DFG (Germany); SFI (Ireland); the Swedish Research Council (Sweden); CAS and CNSF (China); the Alexander von Humboldt Foundation (Germany).

- [a] Visitor from Augustana College, Sioux Falls, SD, USA.
- [b] Visitor from The University of Liverpool, Liverpool, UK.
- [c] Visitor from ECFM, Universidad Autonoma de Sinaloa, Culiacán, Mexico.
- [d] Visitor from II. Physikalisches Institut, Georg-August-University, Göttingen, Germany.
- [e] Visitor from Helsinki Institute of Physics, Helsinki, Finland.
- [f] Visitor from Universität Bern, Bern, Switzerland.
- [g] Visitor from Universität Zürich, Zürich, Switzerland.
- [‡] Deceased.

- [1] ALEPH, DELPHI, L3, and OPAL Collaborations, The LEP Working Group for Higgs Boson Searches, *Phys. Lett. B* **565**, 61 (2003).
- [2] LEP Electroweak Working Group,
<http://lepewwg.web.cern.ch/LEPEWWG/>
- [3] D0 Collaboration, V.M. Abazov *et al.*, *Phys. Rev. Lett.*

- 94**, 091802 (2005).
- [4] D0 Collaboration, V.M. Abazov *et al.*, *Phys. Lett. B* **663**, 26 (2008).
- [5] CDF Collaboration, D. Acosta *et al.*, *Phys. Rev. Lett.* **94**, 091802 (2005).
- [6] CDF Collaboration, T. Aaltonen *et al.*, *Phys. Rev. Lett.* **100**, 041801 (2008).
- [7] D0 Collaboration, V.M. Abazov *et al.*, *Nucl. Instrum. Methods Phys. Res. A* **338**, 185 (1994).
- [8] D0 Collaboration, V.M. Abazov *et al.*, *Nucl. Instrum. Methods Phys. Res. A* **565**, 463 (2006).
- [9] The pseudorapidity is given in terms of the polar angle θ as $\eta \equiv -\ln(\tan \frac{\theta}{2})$, where θ is defined relative to the center of the detector.
- [10] J. Lellouch, FERMILAB-THESIS-2008-36 (2008).
- [11] T. Scanlon, FERMILAB-THESIS-2006-43 (2006).
- [12] G. Blazey *et al.*, arXiv:hep-ex/0005012 (2000).
- [13] D0 Collaboration, V.M. Abazov *et al.*, *Phys. Rev. D* **76**, 092007 (2007).
- [14] T. Sjöstrand *et al.*, *Comput. Phys. Commun.* **135**, 238 (2001), we use version 6.3.
- [15] H.L. Lai *et al.*, *Phys. Rev. D* **55**, 1280 (1997).
- [16] M. Mangano *et al.*, *JHEP* **0307**, 001 (2003).
- [17] A. Pukhov *et al.*, arXiv:hep-ph/9908288 (1999).
- [18] R. Brun and F. Carminati, CERN Program Library Long Writeup W5013, 1993 (unpublished).
- [19] T. Andeen *et al.*, FERMILAB-TM-2365 (2007).
- [20] T. Junk, *Nucl. Instrum. Methods Phys. Res. A* **434**, 435 (1999).
- [21] W. Fisher, FERMILAB-TM-2386-E (2007).
- [22] The TEVNPH Working Group, for the CDF and D0 Collaborations, arXiv:0804.3423 (2008).